UPTEC X 05 037
JUN 2005
ISSN 1401-2138

LINNÉA HOLMÉN

Pharmacological and expressional characterization of G-protein coupled receptors

Master’s degree project

UPPSALA UNIVERSITET

Molecular Biotechnology Programme

Uppsala University School of Engineering

UPTEC X 05 037	**Date of issue 2005-06**

Author

Linnéa Holmén

Title (English)

Pharmacological and expressional characterization of G-protein coupled receptors

Title (Swedish)

Abstract

In two parallel studies, G-protein coupled receptors were studied to determine their pharmacological properties and localization. Real-time reverse transcription PCR was used to localize expression of 15 orphan G-protein coupled receptors within rat brain in preparation for an *in situ* hybridization study. Nine of the receptors showed differential expression in the brain. Four receptors were expressed throughout the brain. Two receptors were not expressed anywhere in the brain.

The interaction of melanocyte stimulating hormones from dogfish with dogfish and human melanocortin receptors was studied using radio-ligand binding and cAMP assay. The ligands bound antagonistically to dogfish receptors and with high affinity to human receptors.

Keywords

Orphan G-protein coupled receptors, melanocortin, radio-ligand binding, real-time PCR

Supervisors

Tatjana Haitina, Robert Fredriksson
Department of Neuroscience, Uppsala University

Scientific reviewer

Anna Kindlundh
Department of Physiology and Pharmacology, The Karolinska Institute

Project name	Sponsors
Language **English**	Security
ISSN 1401-2138	Classification
Supplementary bibliographical information	Pages **35**

Biology Education Centre Biomedical Center Husargatan 3 Uppsala
Box 592 S-75124 Uppsala Tel +46 (0)18 4710000 Fax +46 (0)18 555217

PHARMACOLOGICAL AND EXPRESSIONAL CHARACTERIZATION OF G-PROTEIN COUPLED RECEPTORS

LINNÉA HOLMÉN

Sammanfattning

Kroppens celler kommunicerar genom att utsöndra speciella signalsubstanser (ligander). Dessa binder till mottagarproteiner (receptorer) belägna på andra celler. På så sätt kan cellerna erhålla, delge och vidarebefordra information om vad som pågår i kroppen. För att förstå hur cellerna kommunicerar undersöks var i kroppen en receptorsort finns samt bindningen mellan receptorn och dess ligander. Kunskapen kan användas för att med läkemedel ersätta kommunikationssignaler som saknas eller är felaktiga vid sjukdom.

En viktig receptorsort är de G-protein kopplade receptorerna, som har sin effekt genom att förändra strukturen av så kallade G-proteiner. I detta projekt har två studier gjorts på olika receptorer av denna sort.

I den första studien undersöktes var generna för 15 receptorer uttrycktes i råtthjärnan. En del av receptorerna visades enbart finnas i vissa delar av hjärnan, vilket tyder på att de har specialiserade funktioner. Eftersom väldigt litet är känt om receptorerna är resultaten högintressanta.

Den andra studien gjordes på receptorer som är involverade i signalering rörande födointag. Här studerades mängden ligand som krävs för att bindning ska ske samt huruvida en ligand från pigghaj binder till receptorer i människan. Att liganden visades binda starkt tyder på att generna för liganden och receptorerna inte förändrats särskilt mycket under evolutionens gång.

Examensarbete 20 p inom Molekylär bioteknikprogrammet

Uppsala Universitet, Juni 2005

TABLE OF CONTENTS

ABBREVIATIONS USED

ACTH: adrenocorticotropic hormone
AGRP: agouti-related protein
DFMCx: dogfish melanocortin receptor x
EST: expressed sequence tag
GADPH: glyceraldehyde-3-phosphate dehydrogenase
GPCR: G-protein coupled receptor
hMCx: human melanocortin receptor x
MCR: melanocortin receptor
M-MLV: Moloney murine leukemia virus
MSH: melanocyte stimulating hormone
NDP-MSH: [Nle4, D-Phe7]α-melanocyte stimulating hormone (Nle, norleucine)
POMC: pro-opiomelanocortin
RT-PCR: reverse transcription polymerase chain reaction
SEM: standard error of the mean

INTRODUCTION

2.1 The aims of the studies

The aim of this project was to characterize a number of G-protein coupled receptors (GPCRs) with respect to pharmacological properties and distribution of genetic expression.

2.1.1 Expressional characterization

The aim of this study was to identify which of the GPCRs were expressed in male rat brain and to achieve an overview of the localization this expression. A total of 15 orphan GPCRs, some of which have expressed sequence tags (ESTs), were investigated in nine coronal slices of rat brain, using real-time reverse transcription (RT-) PCR. The study was a preparation for an *in situ* hybridization study with the final aim of deorphanizing the receptors. This study was intended to give a primary indication of the localization of the genes, making an *in situ* hybridization study less labor-intensive.

2.1.2 Pharmacological characterization

The aim was to analyze the affinities of the endogenous ligands to their receptors and show if the activation of the receptors by these ligands resulted in second messenger synthesis, as well as to see how ligands from one organism bound to receptors in a distant relative.

Synthesized melanocyte stimulating hormones (MSHs) from dogfish were studied together with dogfish melanocortin receptors (MCRs), as well as human receptors, to investigate the interactions between the ligands (MSHs) and the receptors.

Radio-ligand binding was used to calculate the affinities of the ligands for the receptors. The activation of the receptors was studied by determining the amount of second messenger synthesized when the ligands were bound.

Dogfish ligand-dogfish receptor and dogfish ligand-human receptor interactions were studied, to give an evolutionary perspective to the receptor-ligand interaction. By comparing binding affinities and second-messenger response, some conclusions could be drawn as to how the genes have evolved, as well as conclusions about the receptor-ligand interaction itself.

2.2 GPCRs

2.2.1 The G-protein coupled receptors

G-protein coupled receptors (see figure 1) are one of the largest groups of proteins in mammals and have many and varying functions in signaling pathways. The term "G-protein" refers to the proteins that couple to the receptors. These proteins bind the guanine (G) nucleotides, GTP and GDP. The G-proteins, which are formed by three distinct parts, associate with the intracellular part of the GPCRs. The receptors are usually located at the cell surface, integrated in the cell membrane.

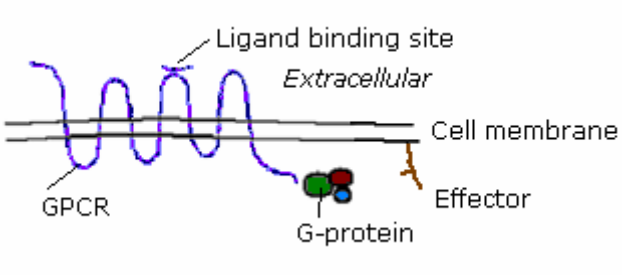

Figure 1: A G-protein coupled receptor. The ligand binds extracellularly. The heterotrimeric G-protein is coupled to the receptor on the inside of the cell membrane. Associated with cell membrane near the receptor is an effector, which will take part in the activation when a ligand has bound the GPCR.

When a ligand binds to the receptor (see figure 2), conformational changes on the inside of the cell membrane lead to dissociation of one of the subunits of the G-protein and thus activation of the G-protein. Depending on which type of G-protein the receptor is associated with, the signal this activation leads to will vary. For example, some receptors are associated with stimulatory G-proteins, while others are associated with inhibitory G-proteins. When a ligand binds to a receptor linked to a stimulatory G-protein, a stimulatory response will follow. The G-protein will dissociate, and one of its trimers will bind to an effector – usually an enzyme. The enzyme will synthesize a second messenger,

for example cyclic AMP or inositol triphosphate. The second messenger will induce the final response in the cell, completing the signaling pathway[1B]. How strong the response will be depends on how much second messenger is synthesized. This, in turn, depends on which ligand and receptor are involved, how strong the interaction between them is, and how many receptors and ligands are present.

In the case of an inhibitory receptor, the effector enzyme will be inhibited, leading to lowered synthesis of the second messenger. Thus, the signaling pathway can be broken. If both a stimulatory and an inhibitory receptor are activated, a pathway can be finely tuned to a certain level of activation.

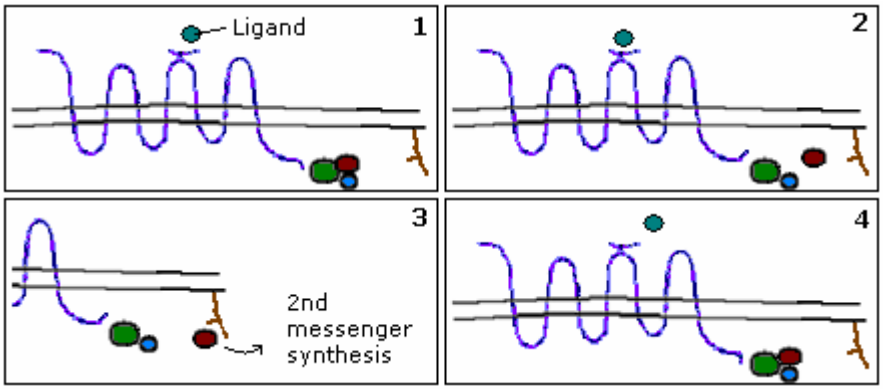

Figure 2: Signaling via a GPCR. The ligand associates with the receptor (1, 2), causing a conformational change in the receptor on the inside of the cell membrane (2), which in turn leads to dissociation of one of the heterotrimers in the G-protein (2). The dissociated G-protein binds to the effector (3), which leads to downstream signals, usually through a 2nd messenger. The ligand dissociates and the G-protein reassociates (4), making the receptor ready for another signaling process.

2.2.2 The GPCR family

The predicted total number of members in the GPCR superfamily lies between 750 and 1000[10]. With so many proteins grouped together, it is not surprising that they have, overall, little in common. In fact, while the family is still commonly referred to as G-protein coupled, for the majority of the receptors no interaction with G-proteins has, as yet, been shown. A better name for the family might be the seven-transmembrane proteins or receptors, as it seems that all GPCRs traverse the cell membrane with seven α-helices[11]. However, the GPCR terminology is more established and therefore remains in use.

Because the GPCR family is so large and diverse, with vital functions in many physiological pathways, it is the topic of much research. About 40-45% of all modern drugs interact with GPCRs in some way, a fact that clearly illustrates how central these receptors are in physiological processes[10].

Each GPCR has a unique expression pattern and each tissue expresses a unique combination of GPCRs[34], making the GPCR system highly useful in targeting specific physiological processes. This can be done through activating a certain combination of the GPCRs, yielding a distinct set of activated pathways. It appears that this same method is used endogenously to achieve tissue- or cell-specificity. Some GPCRs, notably the chemosensory receptors, are only expressed in a single tissue, whereas many endocrine GPCRs are expressed in multiple tissues[34].

It seems that in some cases a GPCR can be involved in, but not crucial to, a given pathway, while another GPCR is vital to the same pathway. Thus, while there would appear to be some functional redundancy in the GPCR family, most receptors seem to have at least one vital function.

It is, in this context, interesting to note that of 367 human endocrine GPCRs, 343 have orthologs among the 392 mouse endocrine GPCRs. Some 50-60 million years have passed since the mouse and human genetic lines diverged[34]. The fact that so many of the receptors have been retained over such a long time period speaks against high redundancy among these receptors. It would be expected that redundant genes would have become pseudogenes or gained new functions, but most endocrine GPCRs have the same function in both human and mouse. The non-redundancy of receptors that appear to have similar functions might be explained by the unique expression pattern of each receptor. Because each receptor is unique in its expression, a receptor that is redundant in one region might be necessary in another.

To identify new GPCRs, the most common method is to search the available completed genome sequences for segments with high sequence similarity to known GPCRs. Many such new receptors are not yet linked to a ligand. These so-called orphan receptors are the target of much research, in the hopes of finding GPCRs with new and interesting functions. The work with identifying new GPCRs has been going on for several years. Due to the immense amount of research put into this field, it is likely that most GPCRs have been identified.

ESTs are tools of prediction of a gene's role and functionality. For orphan GPCRs, the ESTs give a first hint of where the receptor is expressed and hence a suggestion of possible functions, as well as an idea of what kind of future research could and should be performed on that receptor[10].

Another method of identifying possible function is phylogenetic analysis. 60% of GPCRs cluster according to ligand preference, making this a fairly good method of obtaining an indication of possible functions[34].

The novel GPCRs that have been found most recently show a fairly low sequence homology to their relatives[11, 13, 28]. This low homology could suggest that these single copy genes have been under a significant evolutionary pressure to keep their sequences unique. Such genes are rare in the GPCR family, and few of them have known ligands or functions. Their rarity makes prediction of function difficult. It would be highly interesting to identify the ligands and functions of these receptors, as their unique sequences suggest that they have very specialized functions.

2.3 Melanocortin receptor family

2.3.1 The receptors and their ligands

A subfamily of the GPCR superfamily comprises the melanocortin receptors (MCRs). All the receptors in this family are coupled to the stimulatory G_s protein and their activation results in production of cAMP. In mammals there are five melanocortin receptors: MC_1, MC_2, MC_3, MC_4 and MC_5[1].

The ligands for the MCRs, the MSHs, are all produced by posttranslational cleavage of the proopiomelanocortin (POMC) prohormone. The processing of the POMC prohormone is tissue-specific, meaning that the MCR ligands available will vary between tissues. The POMC-system is mainly based in the pituitary gland, with some neurons projecting from the hypothalamus to many diverse brain regions. The derivates of the prohormone are found in all these regions, as well as in the placenta and the gastrointestinal tract. POMC is expressed mainly in the CNS, but also in many peripheral tissues, including skin cells, cells of the immune system, spleen, lung, thyroid, adrenal gland and the gastrointestinal and genitourinary tracts[21]. It is clear that the POMC and its derivates are important in many parts of the body.

The ligands cleaved from the POMC prohormone are in human referred to as ACTH, α-, β- and γ-MSH. A fifth cleavage product, β-endorphin, is also created from the same prohormone. β-endorphin

is not a part of the melanocortin system and is therefore not further mentioned in this report. The amino acid motif His-Phe-Arg-Trp appears in all the MSHs. This sequence is crucial for the ligand-receptor interaction[2].

The hMC_2 receptor binds only ACTH, while other MCR subtypes bind all the MSHs, but with different affinities. NDP-MSH is a very potent agonist of hMC_1, hMC_3, hMC_4 and hMC_5 receptors. α-MSH has the highest affinity for the hMC_1 receptor. γ-MSH is selective for the hMC_3 receptor, but also has high affinity for hMC_1, while it has almost no affinity for hMC_4 and hMC_5. β-MSH has low affinity for hMC_5, but fairly high for the other receptors. α-MSH and ACTH also have a low affinity for hMC_5, compared to hMC_1[1, 12]. A summary of the receptor-ligand interactions in humans is presented in table 1.

Table 1: Receptor-ligand interactions in the melanocortin system in human. The ligands are listed with respect to potency. Parentheses indicate a weak binding. Multiple parentheses indicate a very weak binding.

hMC_1	hMC_2	hMC_3	hMC_4	hMC_5
α-MSH	ACTH	γ-MSH	β-MSH	(ACTH)
ACTH		β-MSH	α-MSH	(α-MSH)
β-MSH		α-MSH	ACTH	((β-MSH))
γ-MSH		ACTH	(((γ-MSH)))	(((γ-MSH)))

The agouti protein and the agouti-related protein (AGRP) are endogenous antagonists of the MCRs[7]. This is unique among the GPCRs - no inhibitory proteins have been identified for other receptors. In mammals agouti binds antagonistically to all the MCRs except the MC_5 receptor, while AGRP binds only the MC_3 and MC_4 receptors[7]. The effects of these interactions are discussed below, in the section covering energy homeostasis. Agouti and AGRP have been studied mainly in mammals, but the peptides have been found in lower vertebrates, such as goldfish, a teleost. However, the effects these molecules have in these species are poorly known.

In the spiny dogfish *Squalus acanthias*, and in other cartilaginous fishes, a fifth endogenous ligand to the melanocortin receptors has been identified, named δ-MSH[2]. The sequences of the ligands suggest that α- and γ-MSH have a common evolutionary ancestor, as do β- and δ-MSH. δ-MSH, found only in cartilaginous fishes, could have arisen from duplication of the β-MSH gene, while γ-MSH might have arisen from a duplication of the α-MSH gene. The sequence of γ-MSH is degenerated or absent in the teleost fishes, but not in sharks such as dogfish. As the teleost fishes are considered evolutionarily higher than the sharks, this suggests that the γ-MSH sequence was present at an early stage in the evolution.

There has been significant genome reorganization among cartilaginous fishes, which is reflected in the different number of MSHs in different species, such as the presence or absence of γ-MSH. Furthermore, it is probably the cause of the varying MCR repertoire among the fishes. In dogfish, for example, three of the five receptor subtypes found in mammals have, as yet, been identified: the MC_3, MC_4 and MC_5 receptors. In the teleost *Fugu*, the MC_3 is lacking, meaning this fish has only four MCR subtypes. In another teleost, zebrafish, the *MC_5 receptor* gene has been duplicated, leading to a sixth receptor type.

The dogfish is the most distant vertebrate relative in which the melanocortin system has been described so far, and it is therefore interesting from an evolutionary point of view. For example, studying the binding of dogfish ligands to human receptors, and *vice versa*, would provide information about how well conserved the melanocortin system is. It would also be interesting to study what

effects, if any, these interactions induce. Such information might help in further elucidating the various functions of the melanocortin system.

The affinity of the human ligands for the dogfish receptors has been previously determined[17, 23]. However, the endogenous dogfish ligands have not been studied before, due to the difficulty of isolating sufficient amounts of ligands for large-scale experiments. By synthesizing the ligands, this problem has been circumvented.

The affinity of δ-MSH for the human receptors has been studied, but with a different sequence than that of the dogfish δ-MSH[24, 25]. The ligand sequence used previously is referred to as Saxon "δ-MSH" throughout this report, Saxon GmbH being the company that provided the peptide (the company has ceased to exist). To determine the affinity of the real δ-MSH for human receptors would be highly interesting, as would elucidation of any effects the interaction might have.

hMC_2 requires a different transfection and expression protocol than the other melanocortin receptors. Furthermore, as it only binds ACTH, it has been considered beyond the scope of this report to study this receptor, especially as concerns its hypothetical binding to δ-MSH. $DFMC_5$ has not yet been successfully expressed and probably also requires a different protocol. Therefore, it has also been excluded from this study. Both these receptors are expressed in intracellular compartments, rather than on the plasma membrane, like the other MCRs.

2.3.2 Effects of the receptor-ligand interactions in mammals

The MC_1 receptor is expressed in melanocytes and many other cell types in skin, as well as in leukocytes[7, 36]. It has a key role in pigmentation. The MC_2 receptor is found in the adrenal gland and in adipose tissue in human. Its main effects are on steroid secretion and through this on, for example, blood pressure and heart rate[1]. The MC_5 receptor has few proven functions and binds with low affinity to most of the known ligands. It is expressed in many peripheral tissues[7, 36].

The MC_3 and MC_4 receptors are both expressed primarily in the brain[7, 36] and involved in energy homeostasis (see the next section). The MC_3 receptor is expressed in some peripheral tissues as well. γ-MSH has a high affinity for MC_3, though what function this serves is unclear. It would appear that the MSHs have some effects on learning and memory. Interestingly, while α-MSH promotes learning, especially from visual cues, γ-MSH seems to have the opposite effect[22].

The MC_4 receptor is involved in sexual function, mainly penile erection and ejaculation[36], but also increases sexual behavior in both genders. This effect is achieved through both α-MSH and ACTH. For males, the effect has been shown in both rodent and human[1]. The effect on females appears far more complex and depends on the levels of progesterone and estrogens, leading to increased *or* decreased sexual behavior. ACTH and α-MSH cause grooming behavior when administered to rats. This is probably mediated through the MC_4 receptor[29].

γ-MSH increases heart rate and blood pressure. Surprisingly, other MC_3 receptor agonists do not have this effect, suggesting either another γ-MSH-binding receptor or a second binding site and activation pathway from the MC_3 receptor. α-MSH has anti-inflammatory and anti-pyretic effects, but it is not clear which receptor induces these responses[7].

2.3.3 MCRs and energy homeostasis in mammals

The MC_3 and MC_4 receptors both have a strong involvement in energy homeostasis. The MC_4 receptor regulates food intake and possibly energy expenditure, the MC_3 receptor influences feeding efficiency and partitioning of fuel stores into fat. Melanocortins promote energy expenditure, leading to a shift towards a negative energy balance[7, 8, 35]. Synthetic agonists of the MC_3 and MC_4 receptors decrease food

intake, while synthetic antagonists increase food intake. Injection of a MC receptor antagonist stimulates feeding, while an injected agonist leads to inhibited feeding, even in fasted mice[3].

The endogenous antagonists agouti and AGRP also influence the metabolism. The synthesis of AGRP is upregulated with fasting and causes hyperphagia[26]. Agouti primarily regulates pigmentation but also appears to be involved in metabolic pathways[7]. The so-called Yellow mouse, a common model for obesity, has a dominant mutation in the promoter for the *agouti* gene leading to overexpression of agouti. This type of mouse has a yellow coat color, is obese and exhibits hyperphagia[19].

Previous studies have indicated that one of the most effective weight loss drugs, d-fenfluramine, induced anorectic effects via melanocortin pathways[14]. This further strengthens the link between the MCRs and energy homeostasis. There is also a large amount of genetic data showing the melanocortin system's influence on the metabolism.

MC_4-receptor knockout mice show the same phenotypical characteristics as the Yellow mice[16]. This may indicate that the connection between agouti and obesity is mediated through MC_4. Interestingly, α-MSH knockout mice exhibit increased feeding as compared to controls. It appears that α-MSH is a potent satiety factor, which works through activating MC_4[26, 35]. If this effect is mediated through MC_4, this could explain the obesity of the MC_4 -/- mice. The same effect would be expected in mice overexpressing agouti and AGRP, as their antagonistic binding causes less α-MSH to bind to the receptors. Thus, it may be that MC_4 -/- mice, Yellow mice and α-MSH -/- mice all become obese due to weakened interaction between α-MSH and MC_4, though through different mechanisms.

MC_4 mutations occur in about 4% of severely obese French individuals[32]. Furthermore, MC_4 deficiency leads to increase in both lean and fat body mass. This is the most common monogenic obesity disorder[31]. Mice lacking one copy of the MC4 receptor gene become obese, but less so than homozygous knockouts[9, 32, 37]. Taken all together, it is clear from these data that the MC_4 is strongly linked to energy homeostasis.

MC_3 -/- mice have smaller lean body mass and more subcutaneous fat than controls, but maintain an approximately normal body weight[5]. Some of the effect of MC_3 may be achieved through illness and aversion. As the phenotype of these mice differs from that of MC_4 -/- mice, it would appear that the receptors have non-redundant functions relating to energy homeostasis.

MC_3 -/- MC_4 -/- double knockout mice have exacerbated obesity as compared to either single knockout strain[8]. This, too, indicates that the receptors are non-redundant as pertains to energy homeostasis. Both MC_3 and MC_4 are expressed in the ventromedial nucleus of the hypothalamus. Lesions in this region of the brain lead to obesity, and the region is considered highly influential in control of feeding behavior[26].

Research done on the ligands of the melanocortin system also suggests strong links to energy homeostasis. POMC neurons have been shown to express leptin receptors[6], suggesting that there is a link between POMC and the peptide leptin, which promotes weight loss. POMC-deficient mice and humans are hyperphagic, obese and resistant to the normal effects of leptin[18, 20]. MC4 -/- mice are also resistant to the effects of leptin, as are Yellow mice.[26]

Leptin-deficient mice display severe obesity and hyperphagia[26]. POMC mRNA expression is reduced in leptin-deficient mice. Administration of leptin to these mice normalizes POMC expression[30]. How these effects are brought about is unclear, but it would appear that there is a definite link between leptin and POMC. The fact that POMC expression is normalized when leptin is injected in leptin-deficient mice may imply that the weight loss effects of leptin are caused by factors encoded in the POMC. For example, one could hypothesize that leptin causes expression of POMC, leading to synthesis of α-MSH and through it, satiety and decreased feeding behavior. The fact that POMC-deficient mice are resistant to leptin supports this hypothesis.

In summary, it is clear that the melanocortin system is heavily involved in energy homeostasis, primarily through the MC_3 and MC_4 receptors, the ligand α-MSH and the antagonists agouti and AGRP.

2.4 Methodology

2.4.1 Real-time PCR & characterization of expression

2.4.1.1 RT-PCR

The quantification of gene expression is highly interesting for many purposes. Identifying if, where and how highly a gene is expressed can indicate gene function or suggest how a certain condition affects an organism's gene expression.

A number of techniques are used to quantify mRNA, including northern blotting, *in situ* hybridization, RNAse protection assays and reverse transcription PCR (RT-PCR). All these techniques have some merit and can be used for different purposes: e.g. *in situ* hybridization allows very precise localization of the mRNA, which the other techniques do not. RT-PCR is the most sensitive of these methods, as well as being more flexible and less time-consuming[4].

RT-PCR uses RNA-dependent DNA polymerases, usually from viral sources, to transcribe mRNA to cDNA, because RNA itself cannot be used as a template in a PCR reaction. The cDNA transcribed can, however, be amplified using the PCR technique.

RT-PCR can be done in one or two steps. In the two-step technique the reverse transcription takes place in one tube, while the PCR-reaction takes place in another. The one-step technique, on the other hand, requires that both polymerases are present in the same tube. Thus, in the two-step technique, a pool of cDNA is created, which is used for PCR amplification, whereas in the one-step method the PCR-reaction includes both transcription of mRNA and amplification of the cDNA created. The one-step method has less risk of contamination, but the two-step method has the strength that the cDNA pool can be stored for later use.

2.4.1.2 Real-time PCR

In the conventional RT-PCR method, the amplified DNA will be further analyzed, usually using gel electrophoresis, Southern blotting and some method for quantitating bands on the gel. Real-time PCR, however, identifies the quantities of DNA simultaneously with the amplification (see figure 3).

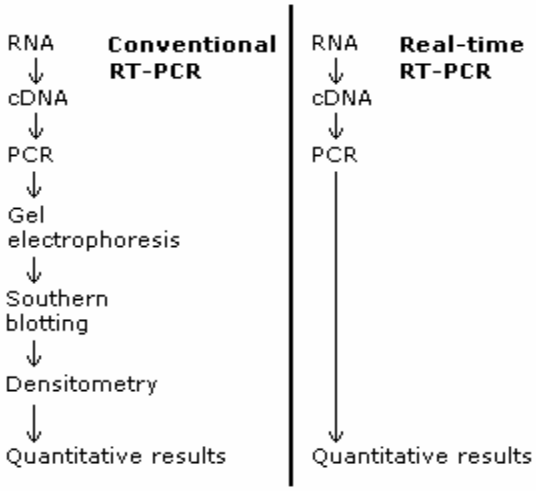

Figure 3: Conventional and real-time RT-PCR. In conventional RT-PCR, several steps are required to obtain quantified results. In real-time RT-PCR, the quantified results are obtained simultaneously with the PCR-reaction. The figure is based upon figure 1 in reference 4.

This real-time quantification is performed using fluorescent dyes that will give a signal only in certain conditions. For example, SYBR Green is a fluorophore that fluoresces only when bound to double-stranded DNA. Therefore, the amount of fluorescence will be in proportion to the amount of dsDNA present at any given time. As the PCR proceeds, fluorescence will increase due to amplification of the DNA of interest (see figure 4). By normalizing the amount of fluorescence yielded when amplifying for the gene of interest, the relative expression of the gene of interest can be determined. The amount of fluorescence yielded from amplification of a gene known to be expressed at a constant level is used as normalization standard.

A threshold point is chosen for a given experiment. This is the cycle during which the fluorescent signal is significantly above the background and here the increase of fluorescence begins to take on an exponential appearance. The number of cycles it takes for a sample to reach the threshold point depends on how much template there is at the beginning of the reaction. Thus, by comparing the number of cycles it takes for samples to reach the threshold point with the same data for negative controls, it is possible to determine if template is present in the samples.

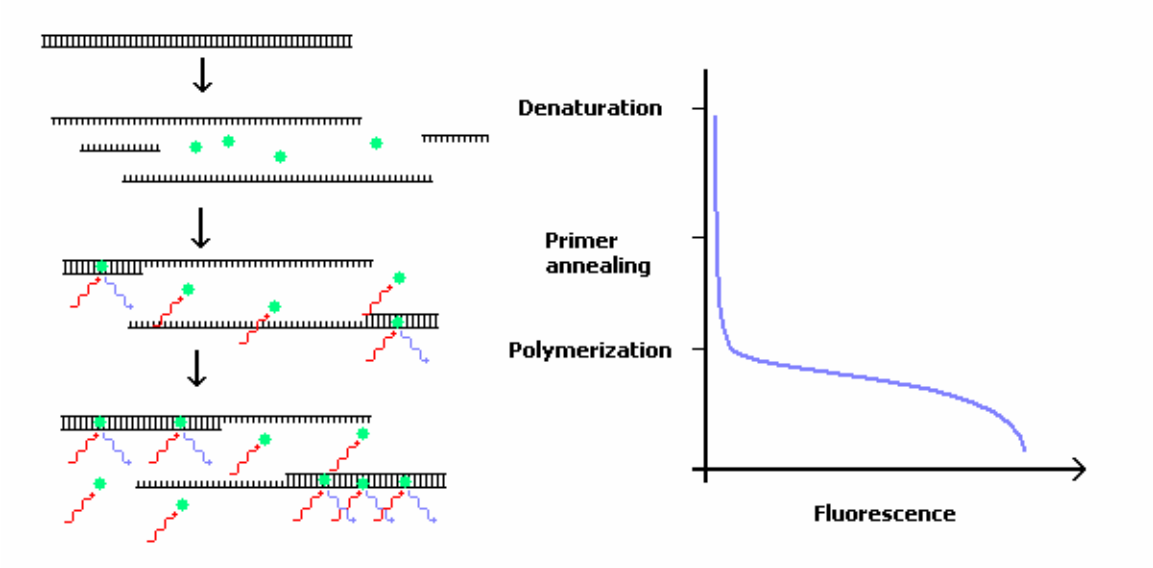

Figure 4. PCR assay using SYBR Green. SYBR Green binds to double-stranded DNA and fluoresces only when bound. Some dye will bind when the primer anneals, leading to a small increase in fluorescence. As the polymerization proceeds, more and more dye binds to the DNA, yielding an increasing fluorescence. The increase of fluorescence, the slope of the curve, will depend on how much template – the target gene – was present at the beginning of the experiment. The point at which the fluorescence first rises significantly above the background is used as a measure of the amount of template. The image is based upon figure 4 in reference 4.

The specificity of this method depends on the specificity of the primers used, as SYBR Green will not differentiate between different sections of dsDNA. To increase the specificity, fluorescence is plotted against temperature, yielding a melting curve. The melting temperature depends on the sequence of the DNA, meaning that it is possible to identify the product of interest. Any contamination will, due to its different DNA-sequence, be visible as a separate peak in the melting curve, making it possible to determine the purity of a reaction.

The main difficulty with the real-time RT-PCR technique, regardless of which fluorophore is used for detection, lies in finding a gene suitable for use as an internal standard, especially if more than one tissue is being studied[4, 33]. Few genes are expressed at constant, or even near-constant, levels between individuals. Still fewer genes are expressed at constant levels between different tissues. Careful

selection of the internal standard, with reference made to the conditions of the experiment and the tissues studied, is critical to the validity of the experiment. Genes commonly chosen as internal standards include glyceraldehyde-3-phosphate dehydrogenase (GADPH) and β-actin. These genes encode moderately common, ubiquitous proteins, which are expressed at nearly constant levels.

In cases where several tissues are being studied or organisms are subjected to different conditions, it is often impossible to select a single gene as an internal standard. This problem is circumvented by studying several reference genes, choosing the most stably expressed and using their geometric average as a normalization factor[33].

2.4.2 Pharmacological characterization

2.4.2.1 Radio-ligand binding

It is often interesting to determine the affinity of a drug or ligand for a receptor. Doing so can help elucidate the function of a receptor or ligand or their joint role in a pathway. The most common method for affinity determination is the radio-ligand binding method, used so often because it is fast, simple and cheap.

In short, a preparation of cells or membranes containing the receptor of interest is exposed to a dilution series of the ligand to be studied and a radioactively marked ligand that competes for the same binding site (see figure 5). The amount of radioactivity the samples show after equilibrium is reached indicates how much of the radioactive ligand has bound[2B]. The amount of radioactivity measured can be plotted against the amount of unlabeled ligand. By varying the amount of unlabeled ligand available, it is possible to construct a so-called competition curve and determine what affinity the ligand has.

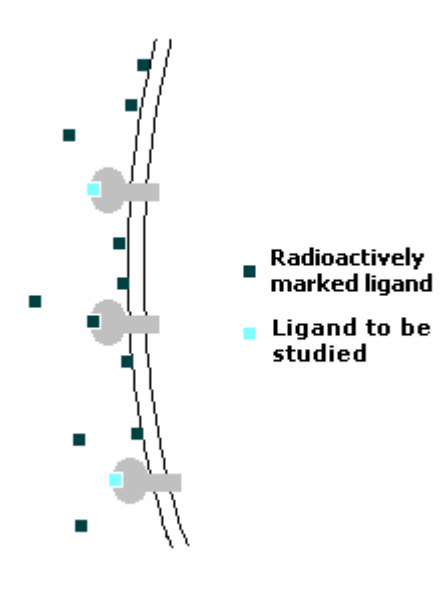

Figure 5: Competition experiment. Cells are incubated with the radiolabeled ligand and the ligand of interest. Bound radioactivity is a measure of how much radiolabeled ligand has bound. By comparing this with the amount of specific binding possible it is possible to determine the affinity of the ligand of interest for the receptor. The image is based upon figure 4:1 in reference 2B.

In order to ensure that the same amount of binding sites is used in binding experiments, it is important to correct for the non-specific binding. This is done in a test binding study. First the total

binding (T) is measured: how much of the radioactive ligand binds when not competing with any other ligand (see panel A, figure 6). Next, the non-specific binding (N) is measured by having the radioactive ligand compete with a very high concentration of a known high-affinity ligand (see panel B, figure 6). The difference between the two (equation (1)) shows how large the largest possible specific binding (S) is.

$$S = T - N \quad (1)$$

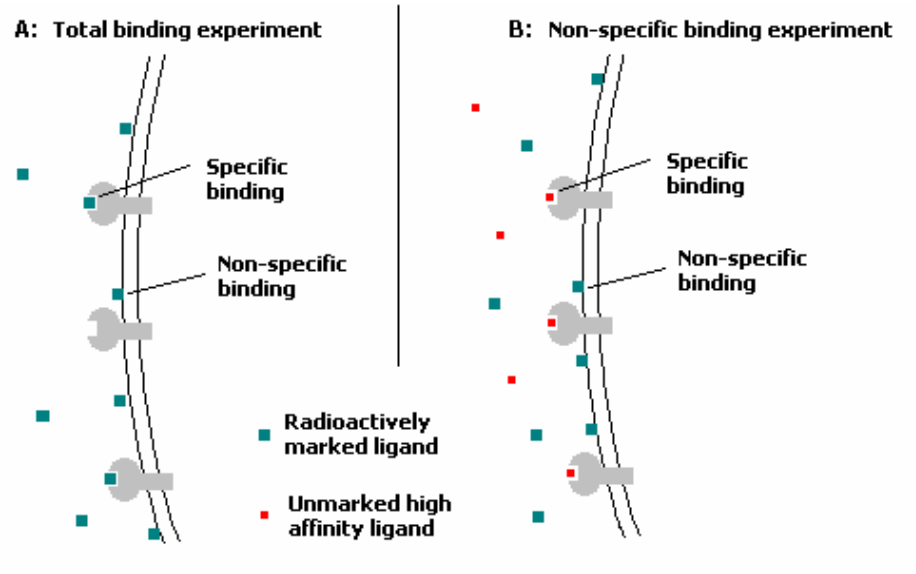

Figure 6. (A.) Total radio-ligand binding experiment. Cells are incubated with the radiolabeled ligand. The amount of radioactivity bound is a measure of the total binding, both specific and non-specific. **(B.)** Non-specific radio-ligand binding experiment. Cells are incubated with the radiolabeled ligand and an unlabeled high affinity ligand. The high affinity ligand will bind all the specific binding sites and the amount of radioactivity bound is a measure of the non-specific binding. By subtracting this from the amount of radioactivity bound in A, a measure of the specific binding is obtained. The image is based upon figure 4:2 in reference 2B.

Plotting the amount of bound radioactive ligand against the concentration of the ligand of interest or "competitor" gives the competition curve. Using Cheng & Prusoff's equation[2B] (2) the dissociation constant of the competitor (K_C or K_i) can be calculated, giving a measure of the competitor's affinity for the receptor.

$$K_C = [C_{50}]^*K_L / ([L] + K_L) \quad (2)$$

Here [L] is the concentration of the radiolabeled ligand, K_L is the dissociation constant of the radiolabeled ligand and $[C_{50}]$ is the concentration of the ligand at which the radioactivity is 50% of what it is when the radiolabeled ligand occupies all the specific binding sites (S in (1)).

A low value of K_C implies that small amounts of the ligand of interest are needed to displace the radiolabeled ligand. This, in turn, indicates that the ligand has a high affinity for the receptor.

2.4.2.2 cAMP assay

Cyclic AMP, cAMP, is a second messenger in the signaling pathways of many GPCRs. When a stimulatory receptor is activated by an agonist, ATP is converted to cAMP, which activates downstream factors and finally leads to an endogenous response. Antagonists block this activation,

meaning that little or no ATP is converted to cAMP and the final response is small or completely absent. An inhibitory receptor will have the opposite characteristics.

The cells are incubated with ATP labeled with tritium (H^3). During incubation, the ATP is incorporated into the cells. After this, the cells are incubated with the ligands that are being studied. At this point varying amounts of radioactively marked ATP will be converted to cAMP. How much cAMP is synthesized depends on whether the ligands are agonists or antagonists, the amount of the ligands and their affinities for the receptors. By measuring the amount of radioactive cAMP synthesized, it is possible to get an idea of the characteristics of the interaction between the ligands and the receptors. Usually, the EC_{50}-value is determined, being the amount of ligand that gives half the maximum cAMP generation of the ligand. A low EC_{50}-value, implying that small amounts of ligand are needed to induce cAMP synthesis, indicates a strong response to the ligand.

Forskolin can be used as a positive control, because it directly activates the adenylate cyclase enzyme, which converts ATP to cAMP. It will give a high yield of cAMP, regardless of receptor interactions.

MATERIALS AND METHODS

3.1 Expressional characterization

Figure 7 shows a diagram of the experimental plan for this study. The rough screening of the rat brain should be followed by a fine screening and an *in situ* hybridization study. Only the rough screening was performed in this study.

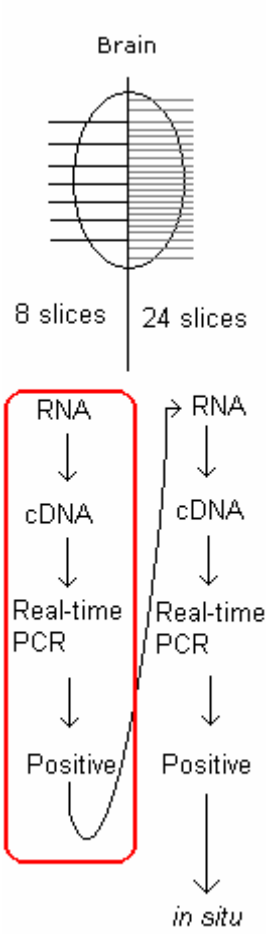

Figure 7. Scheme of the experimental plan for the expressional characterization. The experimental sequence encircled in red was that performed in this study.

3.1.1 Real-time PCR analysis

3.1.1.1 Animal treatment and tissue preparation

For the real-time PCR study, 2 male Sprague-Dawley rats (Alab, Sollentuna, Sweden) were kept in an air-conditioned room (12 h dark/light cycle) at 22 - 23°C and humidity 55%. Initial weight of the animals was 213 ± 1.1 g. The animals had free access to water and R36 food pellets (Labfor, Lactamin, Vadstena, Sweden). After seven days and between three and six hours into the light period, the animals were decapitated and brains were isolated. Each brain was sliced into 24 slices, each of about 1 mm. The slices were divided into two halves. The 24 slices from one of these halves were pooled in groups of three (slices 1-3, 4-6, 7-9, 10-12, 13-15, 16-18, 19-21 and 22-24), resulting in 8 pooled and 24 non-pooled samples. Figure 8 illustrates roughly which regions of the rat brain are part of each slice. The samples were immediately frozen on dry ice and immersed in RNAlater solution (Ambion, USA). The samples were incubated for about 1 h at room temperature, allowing the solution to infiltrate the tissue and then kept in -80°C until further processed. This experimental step was performed by Jonas Lindblom.

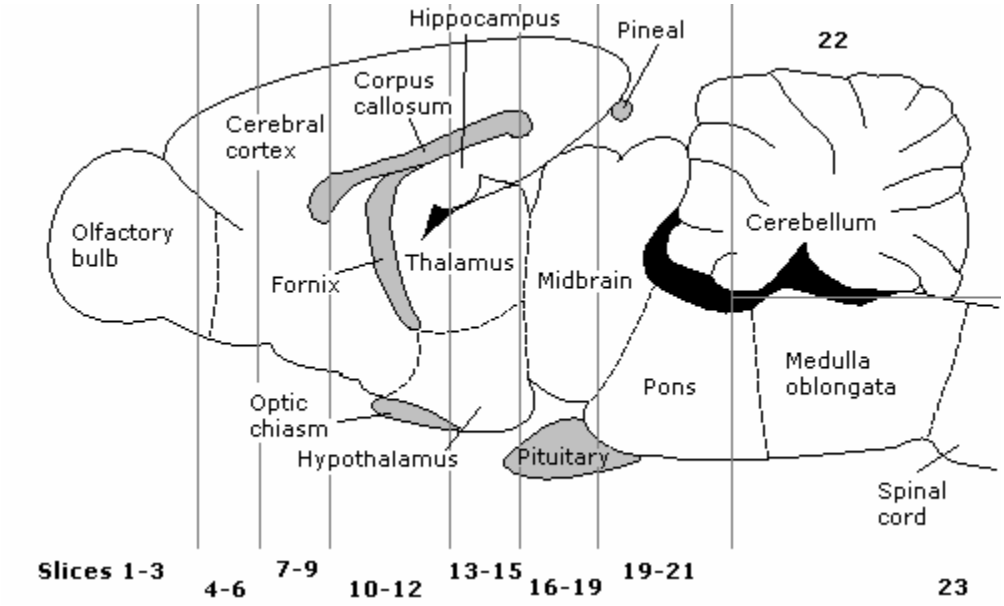

Figure 8: Slicing scheme for the rough screening of orphan GPCRs in the rat brain. Sagittal section of the brain close to the midline. Areas in solid black are the third and fourth ventricles. Boundaries of the brain regions are approximations, as are the boundaries depicting the slicing. The image is based upon the figure 'Lateral 0.40 mm – Sagittal section of the rat brain' from reference 3B.

3.1.1.2 RNA isolation

Tissue samples from one of the sets of pooled brain slices were transferred to tubes with TRIZOL ® Reagent (Invitrogen, Sweden) and kept on ice. The samples were homogenized individually by sonication using a Branson sonifier (Branson Ultrasonics Corporation, Germany). Samples were incubated for > 5 min at room temperature.

Chloroform (0.2 ml per 1 ml TRIZOL) was added to the homogenate and allowed to infiltrate for 2 min at room temperature, followed by centrifugation at 12,000 rpm for 15 min at 4°C. The aqueous phase was transferred to a new tube and RNA was precipitated by adding isopropanol (0.5 ml per 1 ml TRIZOL). Samples were incubated for 10 min at room temperature. After centrifugation at 12,000 rpm for 10 min at 4°C, the pellets were washed twice in 75% ethanol with centrifugation for 5 min at 7500 rpm and 4 °C. The pellets were air dried at room temperature and dissolved in RNAse-free water. DNA contamination was removed by incubating the samples with DNAse for 3 h at 37°C. DNAse was inactivated by incubating the samples for 10 minutes at 75 °C. RNA was stored at -80°C.

The amount of RNA isolated was determined using a NanoDrop® ND-1000 spectrophotometer (NanoDrop Technologies, USA) and the purity of the RNA was checked with PCR (see protocol below). If DNA contamination appeared the DNAse treatment was repeated.

3.1.1.3 cDNA synthesis

10 µg of RNA was mixed with water and incubated at 75°C for 10 min. 4 µl 5x M-MLV Reaction buffer, 2 µl random hexamers (Oligo $(dN)_6$), 1 µl 10 mM dNTP, 200 U M-MLV reverse transcriptase (all from USB Corporation, USA) and RNAse free water were added to each sample, to a final volume of 20 µl. Where the RNA concentration was so low as to necessitate very large volumes (> 20 µl) of RNA, the volumes of the other reagents were adjusted accordingly.

The samples were incubated at 37°C for 1 h, following which the enzyme was denatured by heating the samples to 95°C for 15 min. Finally, water was added to each sample to obtain the cDNA concentration 100 ng/µl. The samples were checked for presence and purity of cDNA using PCR (see below). cDNA was stored at -20°C.

3.1.1.4 Purity control

PCR reactions were mixed according to the following protocol: 1 µl template, 1 µl each of forward and reverse GADPH primers (10 µM; Thermo Electron GmbH, Germany), 0.2 µl Taq DNA polymerase (5 U/µl), 2 µl 10x PCR Rxn Buffer, 0.2 µl dNTP (20 mM), 0.3 µl $MgCl_2$ (all from Invitrogen, Sweden) and autoclaved MQ-H_2O yielding a final volume of 15 µl. A negative control, with MQ-H_2O instead of template, and a positive control, with genomic DNA from rat liver (~100 ng/µl), were also made. The PCR was run for 40 cycles, following a first denaturation at 95°C for 90 s. Each of the cycles contained a denaturation step at 95°C for 30 s, an annealing step at 55°C for 30 s and an extension step at 72 °C for 30 s. A final extension of 5 min at 72 °C followed the last cycle.

Following PCR, samples were run on a 1.5% agarose gel in 0.5x TBE buffer with 3 µl 6x Loading Dye Solution (Fermentas UAB, Lithuania) added to each reaction tube. GeneRuler™ 100 bp DNA ladder Plus (Fermentas UAB, Lithuania) was used to identify the length of the products. The gel was stained in ethidium bromide and bands were observed in UV light.

3.1.1.5 Real-time PCR

5 µl template (5 ng/µl), 0.5 µl each of forward and reverse primers (10 µM; Thermo Electron GmbH, Germany), 0.5 µl SYBR Green (1:50,000; Invitrogen, Sweden) 0.2 µl dNTP (20 mM), 2 µl 10x PCR Rxn Buffer, 0.1 µl Taq DNA polymerase (5 U/µl) 1.6 µl $MgCl_2$ (all from Invitrogen, Sweden) and autoclaved MQ-H_2O were mixed, yielding a final volume of 20 µl. Negative controls were made according to the same protocol, with MQ-H_2O instead of template. A standard curve was made with cDNA in a serial dilution, starting from the concentration used throughout with a dilution factor 1:10 and four final concentrations. GADPH was used as the normalization standard.

Reactions were performed in an iCycler IQ real-time detection instrument (Bio-Rad Laboratories, Sweden). A first denaturation at 95°C for 2 min was followed by 50 identical cycles: denaturation at 95°C for 15 s, annealing at 62°C for 15 s and extension at 72°C for 30 s. After this, the samples were heated from 55°C to 97.5 °C by increments of 0.5°C, each step 10 s, to obtain a melting curve.

All reactions were run in triplicates, with duplicate negative controls for each primer pair. Results were analyzed using the iCycler IQ Optical System Software 3.0a (Bio-Rad Laboratories, Sweden). Where results were inconclusive, reactions were run a second time. If results were still inconclusive, reactions were called negative.

3.2 Pharmacological characterization

3.2.1 Radio-ligand binding

3.2.1.1 Receptor expression

Semi-stable cell lines of EBNA HEK293 (human embryonic kidney) cells, transfected with the receptors of interest ($DFMC_3$, $DFMC_4$, hMC_1, hMC_4), were provided by the supervisor. For cloning and transfection protocol, see e.g. reference 17 (Materials and methods, "Cloning and expression of receptors"). The cells were grown on plates in a humidified environment at 37°C, 5% CO_2 in 10 ml EBNA medium (Dulbecco's modified Eagle's medium; F-12 Nutrient Mixture (D-MEM:F12) with

GlutaMAX I, supplemented with 10% (v/v) fetal bovine serum, 100 u/ml penicillin + streptomycin (PEST), 2.5 µg/ml amphotericin, 250 µg/ml Gibco™ geneticin G-418 (all from Invitrogen, Sweden)). 20 µl of Gibco™ Hygromycin B (50 mg/ml; Invitrogen, Sweden) was added to each plate. After this, the cells were allowed to grow until further used, with fresh medium and antibiotic added every 48 h. When the cells had grown sufficiently, they were detached from the plates and centrifuged for 5 min at 800 rpm. The pellets were resuspended in 400 µl binding buffer (25 mM HEPES buffer (pH 7.4; Eli Lilly, USA), 2.5 mM $CaCl_2$, 1 mM $MgCl_2$ and 0.2% bacitracin) and the solution was frozen at -80°C.

3.2.1.2 Test binding experiments

Total binding was studied by incubating 50 µl of cells (diluted 1:10 in binding buffer) with 25 µl of ^{125}I-labeled NDP-MSH (diluted ~1:140 from assumed stock concentration ~55 nM) and 25 µl binding buffer.

Non-specific binding was analyzed by exposing 50 µl of cells (diluted 1:10 in binding buffer) to 25 µl of unlabeled NDP-MSH (4 µM) and 25 µl ^{125}I-labeled NDP-MSH (diluted ~1:140 from assumed stock concentration ~55 nM).

3.2.1.3 Competition experiments

Ligands were synthesized and supplied by Akiyoshi Takahashi from the Laboratory of Molecular Endocrinology at Kitasato University, Japan.

Serial dilutions of the ligands (α-MSH, β-MSH, γ-MSH, δ-MSH and ACTH) were made from a start concentration of 1 µM, with a dilution factor 1:3 and a total of 12 final ligand concentrations. Dilution was done in binding buffer. Where results indicated a low affinity, the serial dilution in subsequent experiments was started from 10 µM but otherwise identical.

Experiments were performed in a final volume of 100 µl, of which 25 µl were from one of the ligand dilutions, 25 µl were ^{125}I-labeled NDP-MSH (diluted ~1:160 from actual stock concentration ~65 nM) and 50 µl cells (diluted ~1:70 in binding buffer, to obtain 5000 cpm per well, in accordance with specific binding calculations).

3.2.1.4 Analysis of radio-ligand binding

The cells were incubated for 2 h at room temperature. Incubation was terminated by filtration through Filtermat A glass fiber filters (Wallac Oy, Finland) that had been soaked in 0.3% polyethylenimine. Filtration was done using a TOMTEC Mach III cell harvester (Tomtec, USA). After two washes with 5.0 ml of 50mM Tris/HCl (pH 7.5), the filters were dried at 50 °C. MeltiLex A melt-on scintillator sheets (Perkin Elmer, USA) were melted onto the dried filters and radioactivity was counted using a Wallac 1450 (Wizard automatic Microbeta counter, Perkin Elmer, USA). Results were analyzed using GraphPad Prism 3.00 (GraphPad Software, USA).

The assays were performed in duplicate and repeated three to four times. Concentration of the ^{125}I-labeled NDP-MSH was calculated for each experiment.

3.2.1.5 Phylogenetic analysis

Sequences of the dogfish MSHs were obtained from reference 2. Sequences of the human MSHs were found via the Swiss-Prot Database, accession number P01189[1W]. The sequence of the Saxon "δ-MSH" peptide was found in a product catalog from Saxon GmbH. Alignments were made using Clustal W on the EMBL-EBI website[2W], using both individual ligands and the full POMC sequences as raw data. A neighbor-joining tree of the relationships of the ligands was made using the JalView 1.3 beta software.

To study the Saxon "δ-MSH" sequence, BLASTP was used[3W]. The Saxon peptide was used to search for identical sequences in the database.

3.2.2 cAMP assay

3.2.2.1 Receptor expression

Semi-stable cell lines of EBNA HEK293 (human embryonic kidney) cells, transfected with the receptors of interest ($DFMC_3$, $DFMC_4$, hMC_1, hMC_4), were provided by the supervisor. For cloning and transfection protocol, see e.g. reference 17 (Materials and methods, "Cloning and expression of receptors"). The cells were grown on plates in a humidified environment at 37°C, 5% CO_2 in 10 ml EBNA medium (Dulbecco's modified Eagle's medium; F-12 Nutrient Mixture (D-MEM:F12) with GlutaMAX I, supplemented with 10% (v/v) fetal bovine serum, 100 u/ml penicillin + streptomycin (PEST), 2.5 µg/ml amphotericin, 250 µg/ml Gibco™ geneticin G-418 (all from Invitrogen, Sweden)). After 24 h 20 µl of Gibco™ Hygromycin B (50 mg/ml; Invitrogen, Sweden) was added to each plate. After this, the cells were allowed to grow until further used, with fresh medium and antibiotic added every 48 h.

3.2.2.2 Induction of cAMP synthesis

When the cells had grown sufficiently, 25 µl [8-^{3}H]adenine (5 µCi/ml; Amersham Biosciences, Sweden) was added, after which the cells were incubated for ~3 h in normal conditions. Ligands were serially diluted (starting from 20 µM, dilution factor ~1:15, with a total of 6 final ligand concentrations) in cAMP buffer (137 mM NaCl, 5 mM KCl, 0.44 mM KH_2PO_4, 4.2 mM $NaHCO_3$, 1.2 mM $MgCl_2$, 20 mM HEPES, 1 mM $CaCl_2$, 10 mM glucose and 0.5 mM isobutylmethylxanthine (IBMX; Sigma, USA); pH adjusted to 7.4). A plate was prepared with 50 µl of the ligand dilutions and 50 µl of cAMP buffer and incubated at 37°C until further used. A negative control, with only cAMP buffer, and a positive control, with 50 µl of 30 µM forskolin, were also included on the plate.

The cells were harvested in warm IBMX-free cAMP buffer and centrifuged at 800 rpm for 5 min. The pellets, which contained the cells, were resuspended in warm cAMP buffer (50 µl per well + 100 µl extra). The suspension was incubated for 10 min at 37°C. 50 µl of the cell suspension was then added to each well on the plate, after which the plate was incubated for 15 min at 37 °C. The plate was centrifuged for 2 min at 2000 rpm at 4 °C. 200 µl of cold perchloric acid was added to each well and the plate was placed in -20 °C. Each assay was performed in duplicate and repeated once.

3.2.2.3 Isolation of cAMP

Dowex 50 W-X4 resin columns (Bio-Rad Laboratories, Sweden) were washed twice with 10 ml H_2O and placed above scintillation tubes (Zinsser Analytic GmbH, Germany). The plate was thawed at 37 °C and centrifuged at 2000 rpm for 10 min. The supernatants from the wells were added to the Dowex columns. 750 µl PCA (0.33 M) containing ^{14}C-cAMP (600-700 cpm/ml, Amersham Biosciences, Sweden) was also added to each well. The ATP and ADP were eluted with 2x1 ml H_2O. 4 ml OptiPhase 'HiSafe' 3 scintillation fluid (Perkin Elmer, USA) was added to each tube and the tubes were thoroughly shaken using a vortex.

Alumina columns (Sigma, USA) were washed with 8 ml 0.1 M imidazole. The Dowex columns were placed above the Alumina columns, and the cAMP was eluted to the lower columns by addition of 10 ml H_2O. Following this step, the Alumina columns were placed above scintillation tubes. 4 ml 0.1 M imidazole was added to each column to elute the cAMP. 6 ml scintillation fluid was added to each tube and the tubes were shaken using a vortex.

All scintillation tubes were placed in a Tri-carb 1900 CA Packard liquid scintillation beta counter (GMI Inc., USA). Three internal control tubes, containing 750 µl PCA with ^{14}C-cAMP, 4 ml 0.1 M imidazole and 7 ml scintillation fluid were also included in the assay, to obtain a value for the column efficiency. Results were analyzed using GraphPad Prism 3.00 (GraphPad Software, USA). The

conversion of ATP to cAMP was calculated as the percent of eluted [^{3}H]cAMP from total eluted [^{3}H] (cAMP and ATP), corrected against the column efficiency.

RESULTS

4.1 Real-time PCR

The rat brains used were of such morphology that no slice 24 could be isolated. Therefore, slices 22 and 23 were analyzed already in the rough screening.

Results of the screening are presented in table 2 below. As can be seen, GPCRs ***120*** and ***B*** were not expressed in brain at all. GPCRs ***J*** and ***K*** were expressed in all parts of brain. GPCRs ***H***, ***I*** and ***L*** were expressed in almost all parts of the brain. GPCRs ***A***, ***C***, ***E*** and ***G*** were expressed in most, but not all, parts of the brain. GPCRs ***119***, ***D***, ***F*** and ***M*** were expressed in a few, highly localized, regions of the brain. The internal standard used, GADPH, showed sufficiently similar results within and between experiments to justify its use.

Table 2: Results of the real-time RT-PCR screening of orphan GPCRs in Bregma-slices of rat brain. Detection of GPCR expression is denoted with a positive sign (+) and absence of expression with a negative sign (-)

GPCR	119	120	A	B	C	D	E	F	G	H	I	J	K	L	M
Slice 1-3	+	-	+	-	+	-	+	+	+	+	+	+	+	+	+
Slice 4-6	+	-	+	-	+	-	+	-	+	+	+	+	+	+	+
Slice 7-9	-	-	+	-	+	-	+	-	+	+	+	+	+	+	-
Slice 10-12	-	-	-	-	-	-	+	-	-	+	-	+	+	+	-
Slice 13-15	+	-	-	-	-	+	-	-	+	+	+	+	+	+	-
Slice 16-18	-	-	+	-	-	+	-	-	+	+	+	+	+	+	-
Slice 19-21	-	-	+	-	+	+	+	+	+	+	+	+	+	+	+
Slice 22	-	-	+	-	+	+	+	+	+	+	+	+	+	+	+
Slice 23	-	-	+	-	+	-	-	-	-	-	+	+	+	-	-

4.2 Radio-ligand binding

All the ligands bound all the receptors tested. For full results, see table 3. Representative competition curves for all dogfish-receptor-dogfish-ligand interactions are presented in Appendix 1. Representative competition curves for the human-receptor-dogfish-ligand binding experiments, one for each receptor, are presented in figure 9.

Table 3: Dissociation constants (K_i and K_d mean ± SEM) for the dogfish-receptor-dogfish-ligand and human-receptor-dogfish-ligand interactions. ND, not determined. K_d values and data for the Saxon "δ-MSH" taken from references as indicated.

All data in nM	**DFMC3**	**DFMC4**	**hMC1**	**hMC4**
[^{125}I]NDP-MSH (K_d)	0.597 ± 0.007[17]	1.21 ± 0.44[23]	0.0851 ± 0.008[25]	1.78 ± 0.36[24]
ACTH (K_i)	4.511667 ± 0.9414493	23.196 ± 12.94156	ND	ND
α-MSH (K_i)	3.9805 ± 1.8245	645.93 ± 142.79	ND	ND
β-MSH (K_i)	1,091.75 ± 976.25	3,406.667 ± 1,021.15	ND	ND
γ-MSH (K_i)	39.17 ± 21.3387	775.467 ± 212.5551	ND	ND
δ-MSH (K_i)	103.5867 ± 37.4811	216.0333 ± 27.50408	25.2 ± 7.52	419 ± 91.2
"δ-MSH" (K_i)	ND	ND	>30,000[25]	ND

DFMC4 bound ACTH with the highest affinity, while DFMC3 bound α-MSH with the highest affinity. Both receptors bound β-MSH with very low affinity. The human MC4 receptor and the dogfish receptors bound the dogfish δ-MSH with similar affinities. hMC1 bound δ-MSH with much higher affinity than hMC4. In fact, hMC1 has a higher affinity for δ-MSH than either of the dogfish receptors does (see table 3 and the data summary below).

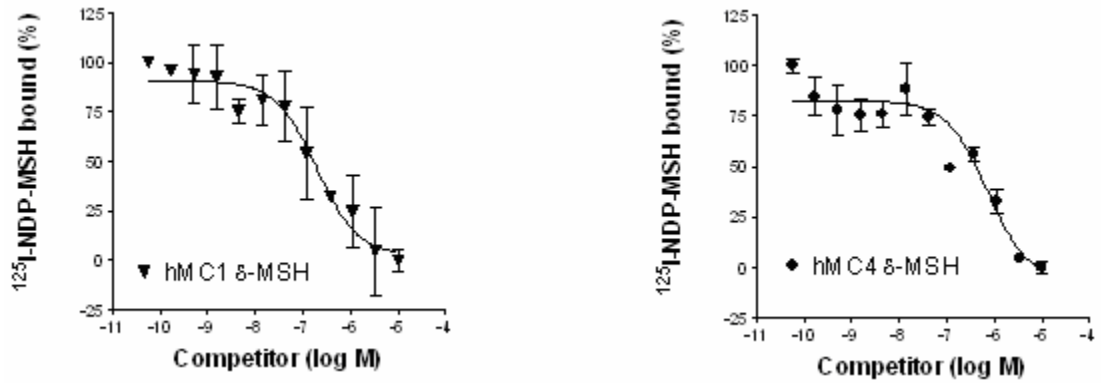

Figure 9: Competition curves for binding of δ-MSH to hMC1 (left curve) and hMC4 (right curve). K_i-values are 32.4 nM for the hMC1-curve and 582 nM for the hMC4-curve.

DFMC3: α-MSH = ACTH > γ-MSH > δ-MSH > β-MSH
DFMC4: ACTH > δ-MSH > α-MSH = γ-MSH > β-MSH
δ-MSH: hMC1 > DFMC4 > DFMC3 > hMC4

Summary of the potency orders determined in the binding experiments. > indicates higher affinity.

The results of the phylogenetic analysis are presented as part of the discussion.

4.3 cAMP assay

The cAMP generation for each receptor-ligand interaction is presented in graphical form in Appendix 2. All receptor-ligand combinations showed induction of cAMP synthesis. The ligands differ somewhat in their potency to activate the cAMP synthesis, with α-MSH being the strongest for both receptors (see table 4). β-MSH showed least activation of cAMP synthesis for $DFMC_3$, while γ-MSH activated $DFMC_4$ most weakly.

Table 4: EC_{50} values for human-receptor-dogfish-ligand interactions.

	$DFMC_4$	**$DFMC_3$**
ACTH	38.0 nM	0.64 nM
α-MSH	0.0036 nM	0.088 nM
β-MSH	10.4 nM	64.9 nM
γ-MSH	237.5 nM	3.86 nM
δ-MSH	47.0 nM	10.1 nM

DISCUSSION

5.1 Expressional localization of GPCRs

The rough screening of rat brain provided important information regarding the localization of the orphan GPCRs. Most interesting are the GPCRs expressed in only some regions of the brain. This could suggest that the GPCRs have an important function in some pathways. As the functions of the GPCRs are unknown, it is impossible to say which pathways they might be involved in. However, with the information given from this rough screening, it will be possible to further localize the GPCRs in question and thereby get an idea of what functions they may have.

For purposes of secrecy, the identities of thirteen of the genes studied have been obscured by encryption. These are referred to as GPR ***A***-***I*** in this text. All receptors except GPR***C*** and GPR***I*** have been found in brain in previous studies. The GPR***120*** and GPR***119*** receptors have been deorphanized recently[15, 27], and have proven functions outside the brain.

The results of the screening study showed that GPR***120*** and GPR***B*** were not expressed at all in rat brain. As it has been recently discovered that GPR***120*** is involved in insulin regulating pathways[15], it is not surprising that this receptor is not found in the brain. The fact that GPR***B*** has been found in rat brain before but was not in this study may be caused by differing expression in the individual animals used.

GPR*J* and GPR*K* were found throughout the brain. Both GPR*L* and GPR*H* were found in all parts of brain except slice 23, the medulla oblongata. GPR*I* was found in all parts except slice 10-12. These receptors probably have one or several important functions in the brain. Interestingly, GPR*I* has not been found in brain before. As in the case of GPR*B*, this discrepancy could be due to differing expression in the animals used in the different experiments.

The seven receptors (GPR*120*, GPR*B*, GPR*H*, GPR*I*, GPR*J*, GPR*K*, and GPR*L*) present or absent in all of or almost all of the brain are least interesting to include in further studies, as they are unlikely to be located at certain pinpoints in the brain. The remaining GPCRs, however, which show some differential localization within the brain, will be highly interesting to proceed with fine screening and *in situ* hybridization.

The GPR*M* receptor was found in slices 19-22, implying that it is expressed in the cerebellum. Similarly, GPR*F* was found in slices 1-3 and 19-22, the olfactory bulb and the cerebellum. These receptors may have more specialized functions than those receptors that were expressed throughout the brain.

GPR*119* was found in slices 1-6 and 13-15. Several brain regions are found there, the major regions being the frontal cortex, the caudate putamen, the globus pallidus, the hippocampus and the hypothalamus. The receptor has been shown to be involved in insulin regulating pathways[27]. This does not exclude the possibility that the receptor has some functions in the brain, which is implied by the fact that it was found expressed in the brain in this study.

GPR*C* was found in the front and back parts of the brain: slices 1-9 and 19-23 – the olfactory bulb, the foremost region of the cortex, the cerebellum and the medulla oblongata. GPR*D* was present in the brain from the hippocampus to the cerebellum (slices 13-22), where major brain regions such as the hippocampus, the hypothalamus, the pituitary and pineal glands and the ventral tegmental area are found. GPR*E*, conversely, was present in the brain up to the hippocampus (slices 1-12), including important regions such as the nucleus accumbens, aside from the first three mentioned in connection with GPR*119*. GPR*E* was also found in the cerebellum (slices 19-22). GPR*C* has not been found in brain before. As previously mentioned, this difference between studies may be due to individual differences in the animals used.

GPCR*A* and GPR*G* were present somewhat erratically throughout the brain. GPR*A* was found in all slices except 10-15. GPR*G* was not present in slices 10-12 and 23.

In this stage it is difficult to hypothesize what specific parts of the brain the differentially expressed receptors might be present in. It may be that the receptors are expressed only in a very small region, such as the substantia nigra, and in one of the neuropeptide pathways, making them appear common throughout the brain, even though their expression is very specific. Such specific localization would make hypothesizing about functions for the receptors possible. For this reason, the fine screening and *in situ* hybridization will be highly interesting, especially as regards these receptors.

The eight receptors (GPR*119*, GPR*A*, GPR*C*, GPR*D*, GPR*E*, GPR*F*, GPR*G*, GPR*M*) showing significant differential expression in the brain will be further analyzed in fine screening and *in situ* hybridization studies. It is to be hoped that this will help elucidate their functions and possible ligands, leading, in the future, to their deorphanization.

Only one gene, GADPH, was used as a standard. This gene is known to be expressed at somewhat varying levels between individuals[4]. While the animals used were matched in all possible respects, there may still be differences in the level of GADPH expression, leading to errors in quantification. However, as this study was solely aimed at identifying expression, rather than quantifying it, the use of a single internal standard is justifiable.

5.2 Pharmacological and evolutionary characterization of GPCRs

5.2.1 Phylogenetic analysis

It has previously been suggested that δ-MSH was created through a duplication of the β-MSH gene[2]. The alignments made in this study indicated some sequence identity supporting this suggestion (see appendix 3). Similarly, α-MSH/ACTH and γ-MSH showed sequence identity, probably arising from another duplication event, as has also been suggested[2]. In human – and in all mammals – only β-MSH exists, implying that the hypothesized gene duplication of β-MSH took place after divergence from the teleosts. It appeared, from this study, that in dogfish, β-MSH has lost its affinity for the MCRs studied, while δ-MSH retained its affinity. The simplest hypothesis suggests that δ-MSH has become the primary ligand, while β-MSH is slowly losing any previous function.

The fact that the identity of dogfish δ-MSH and human β-MSH was shown to be higher than that between dogfish β-MSH and human ditto (see figure 10, panel A, for the alignment and appendix 3 for scores) is highly interesting. Perhaps the nomenclature is faulty, and what is known as δ-MSH in dogfish is the ligand that evolved from the original β-MSH. This would explain the fact that the human β-MSH binds fairly well to dogfish receptors[17], while dogfish β-MSH bound with very low affinity to dogfish receptors, as seen in the binding studies.

Another factor to take into account is the fact that the dogfish δ-MSH sequence is shorter than that of β-MSH in human and dogfish. The important His-Phe-Arg-Trp motif is the N-terminal sequence of δ-MSH, while it is located centrally within the sequences of both β-MSHs. This could mean there is less steric hindrance of the binding of δ-MSH and therefore a higher affinity, as was seen in the binding studies.

It is interesting to note that the "δ-MSH" sequence, from Saxon GmbH had very low scores, especially for the sequences that should be most similar – dogfish β- and δ-MSH. Furthermore, the Saxon "δ-MSH" lacks the important His-Phe-Arg-Trp motif present in all the MSH sequences, with the motif Val-Arg-Gly-Trp instead (see figure 10, panel A). In view of this, neither the low scores in the alignments nor the low affinities of the receptors for this sequence are surprising.

Data mining, using the Saxon "δ-MSH" sequence as a search sequence, returned interesting results. The sequence appeared in the POMC of mammals upstream of the MSHs, as part of what is probably a signaling peptide (see figure 11).

Phylogenetic (neighbor-joining) analysis of the ligands from dogfish and humans grouped the ligands rather than the species (see figure 10, panel B). One would therefore expect that the ligands from one species would bind well to the receptors from the other species, in accordance with the results of this study.

A

```
CLUSTAL W (1.82) multiple sequence alignment


Dfalfa-MSH          -------SYSMEHFRWGKPMG--------------------------
DfACTH              -------SYSMEHFRWGKPMGRKRRPIKVYPNSFEDESSVENMGPEL
Halfa-MSH           -------SYSMEHFRWGKPV---------------------------
HACTH               -------SYSMEHFRWGKPVGKKRRPVKVYPNGAEDESA-EAFPLEF
Saxondelta-MSH      ---------SMEVRGW-------------------------------
Hbeta-MSH           AEKKDEGPYRMEHFRWGSPPKD-------------------------
Dfdelta-MSH         ----DGKIYKMTHFRW-------------------------------
Dfbeta-MSH          ----DGDDYKFGHFRWSVPLKD-------------------------
Hgamma2-MSH         --------YVMGHFRWDR-FG--------------------------
Dfgamma-MSH         -------NYVMGHFRWNK-F---------------------------
```

B

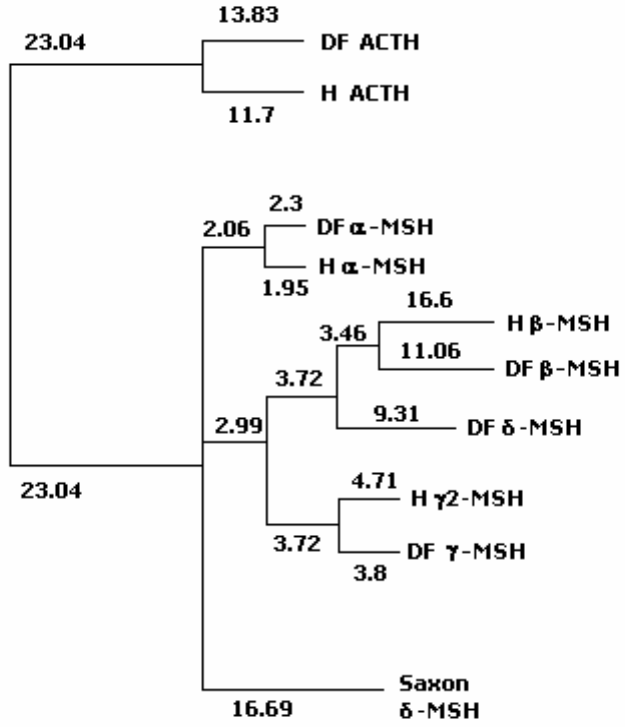

Figure 10. (A.) Alignment of the MSH-ligand sequences constructed using Clustal W. DF = dogfish, H = human. **(B.)** Neighbor-joining tree of the MSH-ligands in humans and dogfish constructed using Clustal W and JalView. "Saxon δ-MSH" is the previously studied δ-MSH ligand (see reference 25). DF = dogfish, H = human.

Figure 11: Alignment of the POMC prohormone sequences from dogfish (df) and humans (hum) constructed using Clustal W. The dogfish ligands are marked in green, the human ligands in magenta. The "δ-MSH" from Saxon GmbH is marked in purple.

5.2.2 Radio-ligand binding

DFMC$_4$ bound all ligands with lower affinity than DFMC$_3$ did. This agrees with previous studies[17] using human ligands and dogfish receptors. Neither the relative order nor the sizes of the affinities agree with previous data for either receptor. While it is not surprising that the K_i-values differ for the binding of dogfish ligands and human ligands to dogfish receptors, the fact that the order of the affinities varies is interesting. This may be due, in part, to the very low affinity of dogfish β-MSH to endogenous receptors, combined with the fairly high affinity of human β-MSH to dogfish receptors.

Dogfish β-MSH bound with very low affinity to both dogfish receptors, while the human β-MSH bound with quite high affinity to the dogfish receptors[17]. Taken together with the fact that δ-MSH bound with a surprisingly high affinity to the human MCRs, this may imply that human β-MSH and dogfish δ-MSH have more in common than either does with dogfish β-MSH. This was confirmed by the phylogenetic data discussed above. It would also explain, to some extent, the differing order of the affinities of the ligands for the receptors. In the human ligand – dogfish receptor study[17], β-MSH bound with a medium affinity, while in this study it bound with a low affinity.

The triplicate experiments agreed quite well with one another, implying that the results were reliable. This is true both for the study with dogfish receptors-dogfish ligands and the study with human receptors-dogfish ligand. In the case of β-MSH binding to DFMC$_3$ the SEM (standard error of the mean) was rather large. This is probably caused by the low affinity of the ligand, placing it close to one of the limits of the interval of ligand concentrations studied, which makes for a large margin of error. It is clear, regardless of the large SEM, that the affinity was quite low, which is the main point of interest.

The human receptor-dogfish ligand study provided very interesting results. As has been mentioned, previous studies used a different "δ-MSH" sequence and the observation in those studies that "δ-MSH" does not bind human receptors is of comparatively little interest, as it is explained by the lack of the His-Phe-Arg-Trp motif. It would appear, from the present study, that δ-MSH did in fact bind the human receptors with similar affinity to that with which it bound the endogenous dogfish receptors. Surprisingly, the human MC_1 receptor bound δ-MSH better than either dogfish receptor.

It would be interesting to proceed with testing of the δ-MSH ligand against the human MC_3 and MC_5 receptors, as well as testing all the dogfish ligands against all the endogenous dogfish MCRs. The relatively high affinity of the δ-MSH for the human receptors, especially hMC_1, raises questions about what responses it causes in human cells. Testing this would also be of high interest.

5.2.3 cAMP assay

All ligands showed an activation of cAMP synthesis. The results are not surprising, as it is well known that the MSHs bind agonistically to the MCRs.

In most cases, the cAMP synthesis did not drop to the level of the negative control. This may indicate that the cells always produce some cAMP, which would lead to a systematic error in the data produced. As the error should be the same for all the ligands, comparing them with one another should be possible. Furthermore, the ligands seldom reached the levels of high synthesis that forskolin reached, suggesting a less-than full activation of the cAMP synthesis. This is, however, to be expected, as few ligands can activate the cAMP synthesis enzyme as strongly as forskolin does.

For some of the receptor-ligand interactions studied the EC_{50} values of the duplicate experiments did not agree. In the case of α-MSH, this was probably due to the very high affinity. As can be seen in the curves (see Appendix 2), the cAMP synthesis did not reach a plateau, even at picomolar concentrations of the ligand. Therefore, the EC_{50} values, calculated as the ligand concentration halfway between the highest and lowest cAMP synthesis levels, did not have a stable lowest level from which they could be calculated. This would have led to large differences in the EC_{50} values. In the case of β-MSH, the discrepancy may have been due to the very low affinity of the ligand for the receptors. When the affinity is on micromolar levels, as it appeared to be for β-MSH, activation of the cAMP synthesis might not occur at all, which could have led to large differences in EC_{50} values.

Because of the discrepancy between the results of the duplicate experiments, it is difficult to compare the activation of cAMP synthesis in response to the different ligands. It is, however, clear that all the ligands were agonists of the MCRs.

For $DFMC_3$, the ligands that bound with high affinity, as seen in the radio-ligand binding study, showed the largest cAMP generation. For example, α-MSH bound with the highest affinity and led to the strongest cAMP response. The relative order of the cAMP generation for the ligands α-MSH, ACTH and γ-MSH agreed with a previous study[17].

For $DFMC_4$, the relative order of the size of the affinity for the ligands did not agree with the relative order of the cAMP generation. However, the fact that the EC_{50} values did not always agree in the duplicate experiments means that it is impossible to say if the EC_{50} values were correct or not. The author was unable to find previous studies of the binding of these ligands to this receptor.

It would be interesting to repeat the cAMP assay a third time, to gain more data on the EC_{50} values of the ligand-receptor interactions. It would also be highly interesting to run a cAMP assay on the interaction between human melanocortin receptors and the dogfish δ-MSH to further study the melanocortin system from an evolutionary perspective.

FINAL NOTES

6.1 Conclusions

6.1.1 Expressional localization

GPR*120*, GPR*B*, GPR*H*, GPR*I*, GPR*J*, GPR*K* and GPR*L* do not appear to have specific localization within the male rat brain. GPR*H*, GPR*I*, GPR*J*, GPR*K*, GPR*L* probably have important functions in the brain, but are expressed in all or almost all regions of it.

The remaining receptors are differentially expressed within the male rat brain, implying that they have specialized functions.

6.1.2 Pharmacological characterization

δ-MSH binds both dogfish and human melanocortin receptors. It binds with highest affinity to the hMC_1 receptor.
All the dogfish ligands bind agonistically to the dogfish receptors studied. β-MSH has the lowest affinity. This, together with the relatively high affinity of δ-MSH to the dogfish receptors, and the phylogenetic data indicating a common ancestor for these two ligands, suggests that β-MSH is losing its affinity and, perhaps, its function, while δ-MSH is taking over as the primary ligand.

6.2 Future Perspectives

6.2.1 Expressional localization

GPR*120*, GPR*B*, GPR*H*, GPR*I*, GPR*J*, GPR*K* and GPR*L* will not be further analyzed in rat brain. Other methods, such as phylogenetic analysis, could be used to identify their functions.

The other GPRs will be analyzed using the finer slices prepared. Those regions where expression of the GPRs is indicated will be further analyzed in an *in situ* hybridization study.

6.2.2 Pharmacological characterization

hMC_3 and hMC_5 should be tested in regards to their affinity to δ-MSH. The response in human cells to the binding of δ-MSH to each of the human receptors should be analyzed. It would also be highly interesting to study the function of δ-MSH in dogfish.

ACKNOWLEDGEMENTS

A general thanks to everyone of Helgi Schiöth's, Klas Kullander's, Dan Larhammar's and Lars Oreland's groups for being helpful in the lab and creating a pleasant atmosphere in the department. Thanks to Helgi Schiöth, Robert Fredriksson, Chris Pickering, Lotta Avesson and Jesper Gantelius for providing help, support and inspiration.

Special thanks to Akiyoshi Takahashi of the Laboratory of Molecular Endocrinology at Kitasato University, Japan for synthesizing dogfish MSHs and to Jonas Lindblom for animal handling, providing Bregma-slices of rat brain, as well as being helpful around the lab and at meetings. Also thanks to Björn Karlsson for permission to use his photographs of spiny dogfish in the oral presentation.

Thanks to my scientific reviewer, Anna Kindlundh, for all her kind help.

Lastly, my sincerest thanks are directed to Tatjana Haitina for her helpfulness, kindness and understanding in supervising my work.

REFERENCES

Scientific articles:

1. Adan, R.A.H. & Gispen, W. H., Brain Melanocortin Receptors: From Cloning to Function. *Peptides* (1997) **18**: 1279-1287.

2. Amimeya, Y., Takahashi, A., Suzuki, N., Sasayama, Y. & Kawauchi, H., A Newly Characterized Melanotropin in Proopiomelanocortin in Pituitaries of an Elasmobranch, *Squalus acanthias*. *General and Comparative Endocrinology* (1999) **114**: 387-395.

3. Benoit, S.C., Schwartz, M.W., Lachey, J.L., Hagan, M.M., Rushing, P.A., Blake, K.A., Yagaloff, K.A., Kurylko, G., Franco, L., Danhoo, W., & Seeley, R.J., A Novel Selective Melanocortin-4 Receptor Agonist Reduces Food Intake in Rats and Mice without Producing Aversive Consequences. *Journal of Neuroscience* (2000) **20**: 3442-3448.

4. Bustin, S.A., Absolute quantification of mRNA using real-time reverse transcription polymerase chain reaction assays. *Journal of Molecular Endocrinology* (2000) **25**: 169-193.

5. Chen, A.S., Marsh, D.J., Trumbauer, M.E., Frazier, E.G., Guan, X., Yu, H., Rosenblum, C.I., Vongs, A., Feng, Y., Cao, L., Metzger, J.M., Strack, A.M., Carnacho, R.E., Mellin, T.N., Nunes, C.N., Min, W., Fisher, J., Gopal-Truter, S., MacIntyre, D.E., Chen, H.Y. & Van der Ploeg, L.H.T., Inactivation of the mouse melanocortin-3 receptor results in increased fat mass and reduced lean body mass. *Nature Genetics* (2000) **26**: 97-102.

6. Cheung, C.C., Clifton, D.K. & Steiner, R.A., Proopiomelanocortin Neurons are Direct Targets for Leptin in the Hypothalamus. *Endocrinology* (1997) **138**: 4489-4492.

7. Cone, R.D., The Central Melanocortin System and Energy Homeostasis. *Trends in Endocrinology and Metabolism* (1999) **10**: 211-216.

8. Cummings, D.E. & Schwartz, M.W., Melanocortins and body weight: a tale of two receptors. *Nature Genetics* (2000) **26**: 8-9.

9. Farooqi, I.S., Keogh, J.M., Yeo, G.S.H., Lank, E.J., Cheetham, T. & O'Rahilly, S., Clinical Spectrum of Obesity and Mutations in the Melanocortin 4 Receptor Gene. *The New England Journal of Medicine* (2003) **348**: 1085-1095.

10. Fredriksson, R., Höglund, P.J., Gloriam, D.E.I., Lagerström, M.C. & Schöith, H.B., Seven evolutionarily conserved human rhodopsin G protein-coupled receptors lacking close relatives. *FEBS Letters* (2003) **554**: 381-388.

11. Fredriksson, R., Lagerström, M.C., Lundin, L. & Schiöth, H.B., The G-Protein Coupled Receptors in the Human Genome Form Five Main Families. Phylogenetic Analysis, Paralogon Groups, and Fingerprints. *Molecular Pharmacology* (2003) **63**: 1256-1272.

12. Gantz, I. & Fong, T.M., The Melanocortin system. *American Journal of Physiology. Endocrinology and metabolism.* (2003) **284**: E468-E474.

13. Gloriam, D.E.I., Schiöth, H.B. & Fredriksson, R., Nine new human Rhodopsin family G-protein coupled receptors: identification, sequence characterisation and evolutionary relationship. *Biochimica et Biophysica Acta – General Subjects* (2005) **1722**: 235-246.

14. Heisler, L.K., Cowley, M.A., Tecott, L.H., Fan, W., Low, M.J., Smart, J.L., Rubinstein, M., Tatro, J.B., Marcus, J.N., Holstege, H., Lee, C.E., Cone, R.D. & Elmquist, J.K., Activation of Central Melanocortin Pathways by Fenfluramine. *Science* (2002) **297**: 609-611.

15. Hirasawa, A., Tsumaya, K., Awaji, T., Katsuma, S., Adachi, T., Yamada, M., Sugimoto, Y., Miyazaki, S. & Tsujimoto, G., Free fatty acids regulate gut incretin glucagon-like peptide-1 secretion through GPR120. *Nature Medicine* (2005) **11**: 90-94.

16. Huszar, D., Lynch, C.A., Fairchild-Huntress, V., Dunmore, J.H., Fang, Q., Berkemeier, L.R., Gu, W., Kesterson, R.A., Boston, B.A., Cone, R.D., Smith, F.J., Campfield, L.A., Burn, P. & Lee, F., Targeted Disruption of the Melanocortin-4 Receptor Results in Obesity in Mice. *Cell* (1997) **88**: 131-141.

17. Klovins, J., Haitina, T., Ringholm, A., Löwgren, M., Fridmanis, D., Slaidina, M., Stier, S. & Schiöth, H.B., Cloning of two melanocortin (MC) receptors in spiny dogfish. *European Journal of Biochemistry* (2004) **271**: 4320-4331.

18. Krude, H., Beibermann, H., Luck, W., Horn, R., Brabant, G. & Grüters, A., Severe early-onset obesity, adrenal insufficiency and red hair pigmentation caused by POMC mutations in humans. *Nature Genetics* (1998) **19**: 155-157.

19. Michaud, E.J., Mynatt, R.L., Miltenberger, R.J., Klebig, M.L., Wilkinson, J.E., Zemel, M.B., Wilkison, W.O. & Woychik, R.P., Obesity and the Adipocyte. Role of the *agouti* gene in obesity. *Journal of Endocrinology* (1997) **155**: 207-209.

20. Mountjoy, K.G. & Wong, J., Obesity, Diabetes and Functions for Proopiomelanocortin-derived Peptides. *Molecular and Cellular Endocrinology* (1997) **128**: 171-177.

21. O'Donohue, T.L. & Dorsa, D. M., The Opiomelanotropinergic Neuronal and Endocrine systems. *Peptides* (1982) **3**: 353-395.

22. O'Donohue, T.L., Handelmann, G.E., Lop, Y.P., Olton, D.S., Leibowitz, J. & Jacobowitz, D.M., Comparison of biological and behavioral activities of alpha- and gamma-melanocyte stimulating hormones. *Peptides* (1981) **2**: 101-104.

23. Ringholm, A., Klovins, J., Fredriksson, R., Poliakova, N., Larson, E.T., Kukkonen, J.P., Larhammar, D. & Schiöth, H.B., Presence of melanocortin (MC4) receptor in spiny dogfish suggests an ancient vertebrate origin of central melanocortin system. *European Journal of Biochemistry* (2003) **270**: 213-221.

24. Schiöth, H.B., Bouifrouri, A.A., Rudzish, R., Muceniece, R., Watanobe, H., Wikberg, J.E.S. & Larhammar, D., Pharmacological comparison of rat and human melanocortin 3 and 4 receptors in vitro. *Regulatory Peptides* (2002) **106**: 7-12.

25. Schiöth, H.B., Muceniece, R., Wikberg, J.E.S. & Chhajlani, V., Characterisation of melanocortin receptor subtypes by radio-ligand binding analysis. *European Journal of Pharmacology. Molecular Pharmacology* Section (1995) **288**: 311-317.

26. Schwartz, M.W., Woods, S.C., Porte Jr., D., Seeley, R.J. & Baskin, D.G., Central nervous system control of food intake. *Nature* (2000) **404**: 661-671.

27. Soga, T., Ohishi, T., Matsui, T., Saito, T., Matsumoto, M., Takasaki, J., Matsumoto, S., Kamohara, M., Hiyama, H., Yoshida, S., Momose, K., Ueda, Y., Matsushime, H., Kobori, M. & Furuichi, K., Lysophosphatidylcholine enhances glucose-dependent insulin secretion via an orphan G-protein-coupled receptor. *Biochemical and Biophysical Research Communications* (2005) **326**: 744-751.

28. Takeda, S., Kadowaki, S., Haga, T., Takaesu, H. & Mitaku, S., Identification of G protein-coupled receptors genes from the human genome sequence. *FEBS Letters* (2002) **520**: 97-101.

29. Thody, A.J., Wilson, C.A. & Everard, D., Facilitation and Inhibition of Sexual Receptivity in the Female Rat by α-MSH. *Physiology & Behavior* (1979) **22**: 447-450.

30. Thornton, J.E., Cheung, C.C., Clifton, D.K. & Steiner, R.A., Regulation of Hypothalamic Proopiomelanocortin mRNA by Leptin in ob/ob mice. *Endocrinology* (1997) **138**: 5063-5066.

31. Vaisse, C., Clement, K., Durand, E., Hercberg, S., Guy-Grand, B. & Froguel, P., Melancortin-4 receptor mutations are a frequent and heterogeneous cause of morbid obesity. *Journal of Clinical Investigation* (2000) **106**: 253-262.

32. Vaisse, C., Clement, K., Guy-Grand, B. & Froguel, P., A frameshift mutation in human MC4R is associated with a dominant form of obesity. *Nature Genetics* (1998) **20**: 113-114.

33. Vandersompele, J., De Preter, K., Pattyn, F., Poppe, B., Van Roy, N., De Paepe, A. & Speleman, F., Accurate normalization of real-time quantitative RT-PCR data by geometric averaging of multiple internal control genes. *Genome Biology* (2002) **3**: research0034.1-0034.11.

34. Vassilatis, D.K., Hohmann, J.G., Zeng, H., Li, F., Ranchalis, J.E., Mortrud, M.T., Brown, A., Rodriguez, S.S., Weller, J.R., Wright, A.C., Bergmann, J.E. & Gaitanaris, G.A., The G protein-coupled receptor repertoires of human and mouse. *Proceedings of the National Academy of Science of the United States of America* (2003) **100**: 4903-4908.

35. Vergoni, A.V., Schiöth, H.B. & Bertolini, A., Melanocortins and feeding behavior. *Biomedicine and Pharmacotherapy* (2000) **54**: 129-134.

36. Wikberg, J.E.S., Melanocortin receptors: perspectives for novel drugs. *European Journal of Pharmacology* (1999) **375**: 295-310.

37. Yeo, G.S.H., Farooqi, I.S., Aminian, S., Halsall, D.J., Stanhope, R.G. & O'Rahilly, S., A frameshift mutation in MC4R associated with dominantly inherited human obesity. *Nature Genetics* (1998) **20**: 111-112.

Other literature:

1B. Mathews, C.K., van Holde, K.E. & Ahern, K.G., Biochemistry, Third Edition (2000), Addison Wesley Longman, Inc., San Francisco.

2B. Wikberg, J., Farmakologiska grundprinciper (2004).

3B. Paxinos, G. & Watson, C., The Rat Brain in Stereotaxic Coordinates, Compact Third Edition (1997), Academic Press, Inc., Sydney.

Websites:

1W. Swiss-Prot, The Protein Knowledgebase, Human POMC entry: http://www.expasy.org/uniprot/P01189 (May, 2005).

2W. Clustal W: http://www.ebi.ac.uk/clustalw/ (April, 2005).

3W. BLAST, The Basic Local Alignment Search Tool: http://www.ncbi.nlm.nih.gov/blast/ (April, 2005).

Appendix 1: Representative competition curves for receptor-ligand interactions of dogfish receptors MC3 and MC4 and dogfish ligands ACTH, α-, β-, γ- and δ-MSH

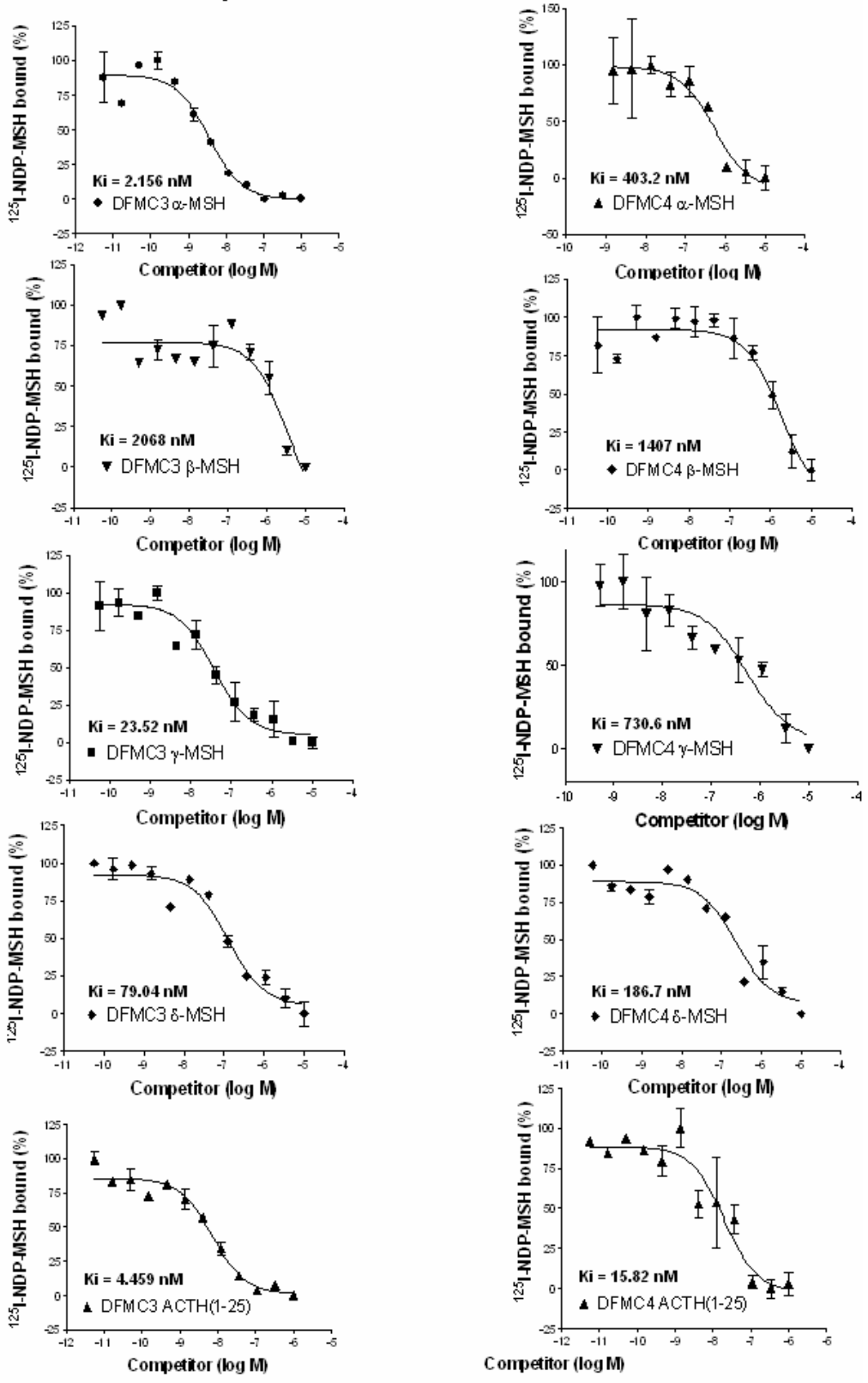

Appendix 2: cAMP generation for receptor-ligand interaction of dogfish receptor MC3 and MC4 and dogfish ligands ACTH, α-, β-, γ- and δ-MSH

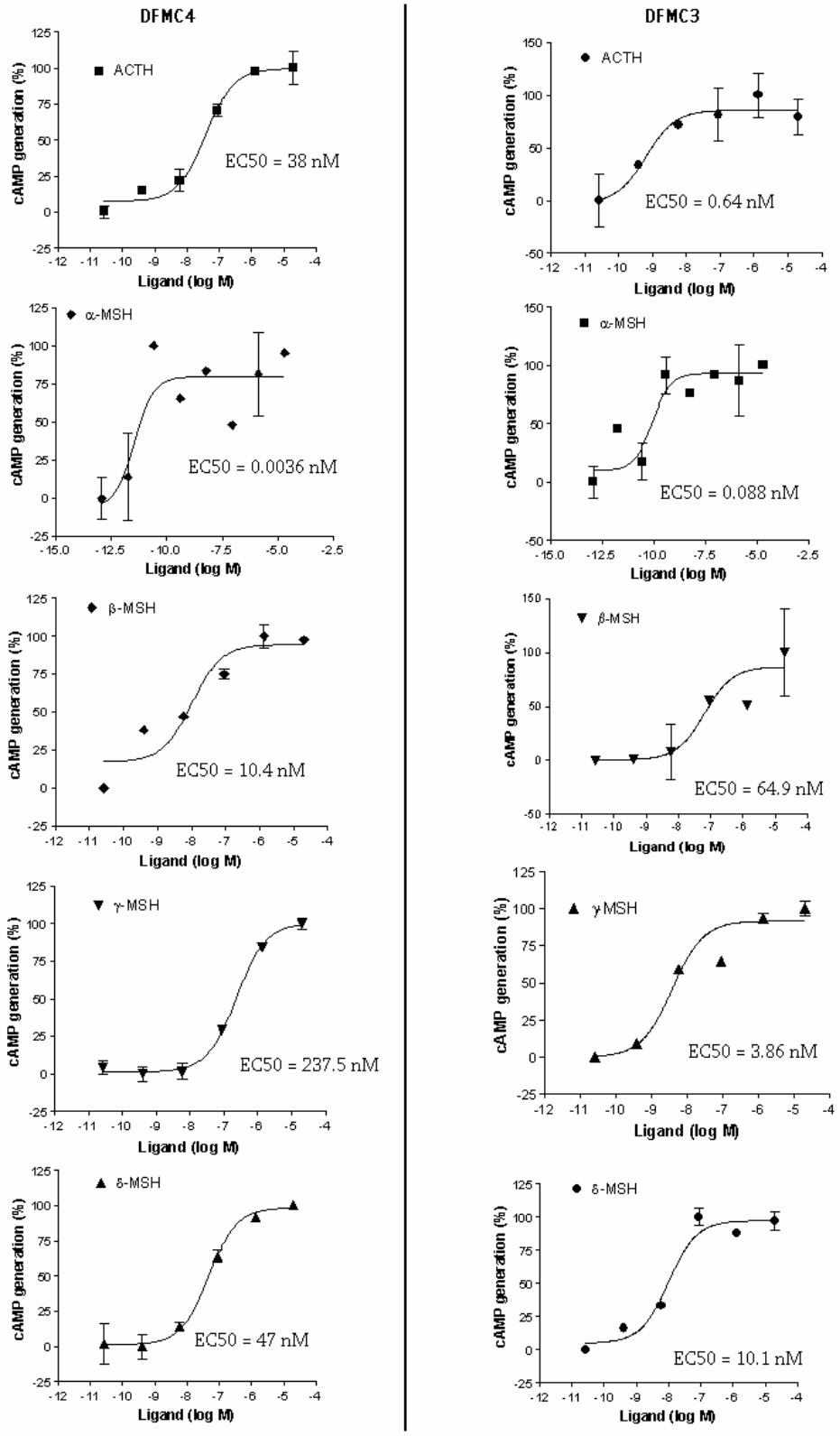

Appendix 3

Scores for the ClustalW multiple sequence alignment of melanocyte stimulation hormones (ACTH, α-, β-, γ-MSH) from dogfish and humans, δ-MSH from dogfish and "δ-MSH" from Saxon GmbH.

Df = dogfish. H = human.

SeqA	Name	Len(aa)	SeqB	Name	Len(aa)	Score
1	Dfdelta-MSH	12	2	Saxondelta-MSH	7	14
1	Dfdelta-MSH	12	3	Halfa-MSH	13	50
1	Dfdelta-MSH	12	4	Dfalfa-MSH	14	50
1	Dfdelta-MSH	12	5	Hbeta-MSH	22	58
1	Dfdelta-MSH	12	6	Dfbeta-MSH	18	66
1	Dfdelta-MSH	12	7	Hgamma2-MSH	12	50
1	Dfdelta-MSH	12	8	Dfgamma-MSH	12	50
1	Dfdelta-MSH	12	9	HACTH	39	50
1	Dfdelta-MSH	12	10	DfACTH	40	50
2	Saxondelta-MSH	7	3	Halfa-MSH	13	57
2	Saxondelta-MSH	7	4	Dfalfa-MSH	14	57
2	Saxondelta-MSH	7	5	Hbeta-MSH	22	42
2	Saxondelta-MSH	7	6	Dfbeta-MSH	18	14
2	Saxondelta-MSH	7	7	Hgamma2-MSH	12	14
2	Saxondelta-MSH	7	8	Dfgamma-MSH	12	14
2	Saxondelta-MSH	7	9	HACTH	39	57
2	Saxondelta-MSH	7	10	DfACTH	40	57
3	Halfa-MSH	13	4	Dfalfa-MSH	14	92
3	Halfa-MSH	13	5	Hbeta-MSH	22	69
3	Halfa-MSH	13	6	Dfbeta-MSH	18	46
3	Halfa-MSH	13	7	Hgamma2-MSH	12	50
3	Halfa-MSH	13	8	Dfgamma-MSH	12	58
3	Halfa-MSH	13	9	HACTH	39	100
3	Halfa-MSH	13	10	DfACTH	40	92
4	Dfalfa-MSH	14	5	Hbeta-MSH	22	64
4	Dfalfa-MSH	14	6	Dfbeta-MSH	18	42
4	Dfalfa-MSH	14	7	Hgamma2-MSH	12	50
4	Dfalfa-MSH	14	8	Dfgamma-MSH	12	58
4	Dfalfa-MSH	14	9	HACTH	39	92
4	Dfalfa-MSH	14	10	DfACTH	40	100
5	Hbeta-MSH	22	6	Dfbeta-MSH	18	50
5	Hbeta-MSH	22	7	Hgamma2-MSH	12	50
5	Hbeta-MSH	22	8	Dfgamma-MSH	12	50
5	Hbeta-MSH	22	9	HACTH	39	40
5	Hbeta-MSH	22	10	DfACTH	40	40
6	Dfbeta-MSH	18	7	Hgamma2-MSH	12	50
6	Dfbeta-MSH	18	8	Dfgamma-MSH	12	50
6	Dfbeta-MSH	18	9	HACTH	39	33
6	Dfbeta-MSH	18	10	DfACTH	40	33
7	Hgamma2-MSH	12	8	Dfgamma-MSH	12	75
7	Hgamma2-MSH	12	9	HACTH	39	50
7	Hgamma2-MSH	12	10	DfACTH	40	50
8	Dfgamma-MSH	12	9	HACTH	39	58
8	Dfgamma-MSH	12	10	DfACTH	40	58
9	HACTH	39	10	DfACTH	40	66